# Trapped ion effect on shielding, current flow, and charging of a small object in a plasma

Mártin Lampe[a)]
*Plasma Physics Division, Naval Research Laboratory, Washington, D.C. 20375-5346*

Rajiv Goswami
*Institute for Research in Electronics and Applied Physics, University of Maryland, College Park, Maryland 20740*

Zoltan Sternovsky and Scott Robertson
*Physics Department, University of Colorado, Boulder, Colorado 80309-0390*

Valeriy Gavrishchaka
*Science Applications International Corporation, McLean, Virginia 22101*

Gurudas Ganguli and Glenn Joyce
*Plasma Physics Division, Naval Research Laboratory, Washington, D.C. 20375-5346*

(Received 15 August 2002; accepted 28 January 2003)

The problem of electrostatic shielding around a small spherical collector immersed in nonflowing plasma, and the related problem of electron and ion flow to the collector, date to the origins of plasma physics. Calculations have typically neglected collisions, on the grounds that the mean free path is long compared to the Debye length. However, it has long been suspected that negative-energy trapped ions, created by occasional collisions, could be important. This paper presents self-consistent analytic calculations of the density and distribution function of trapped and untrapped ions, the potential profile, the ion and electron current to the collector, and the floating potential and charge of the collector. Under typical conditions for dust grains immersed in a discharge plasma, trapped ions are found to dominate the shielding near the grain, substantially increase the ion current to the grain, and suppress the floating potential and grain charge, even when the mean free path is much greater than the Debye length. © *2003 American Institute of Physics.* [DOI: 10.1063/1.1562163]

## I. INTRODUCTION

When a small object is immersed in plasma, both electrons and positive ions flow to the object and are absorbed on its surface. If the object is electrically floating, it will acquire a negative charge, due to more rapid bombardment by electrons than by ions. In recent years, there has been a great deal of interest in the physics of dusty plasmas, i.e., plasmas that contain many particulates (''dust grains'') with radii that are small compared to the Debye length. In typical laboratory experiments, particulate sizes are 1–10 $\mu$m, and the grain charge is on the order of thousands of electron charges. A variety of interesting collective behaviors occur because of the very strong plasma-mediated interaction between dust grains. However the most fundamental issue of dusty plasma physics is the response of the plasma to the presence of a single dust grain, i.e., the shielding around the charged grain, the electron and ion current to the grain, and the steady state floating potential and charge on the grain. Analyses of dusty plasma[1–8] have drawn on the theories developed in earlier times for Langmuir probes and spacecraft charging.[9–15] This body of work comprises an enormous literature, beginning with Langmuir and collaborators[9] in the 1920s, followed by many classic papers. Theoretical work on dusty plasma has most often assumed that (if there is no plasma streaming relative to the dust grains) the charge and shielding of each grain are given by the orbital-motion-limited (OML) theory,[1–6,9,11–16] or by simpler approximations to the OML result such as the Debye-shielded potential.

OML theory, and nearly all of the theoretical treatments dating back to Langmuir,[9] neglect collisions in treating the plasma response near the object. This would seem to be quite a reasonable assumption, since the mean free paths for collisional processes are typically long compared to the Debye length (the characteristic length of the shielding cloud around the object) in laboratory, space, and astrophysical plasmas. If the plasma is collisionless, then ions coming in toward the object from the ambient plasma will either contact the object (in which case it is usually assumed they are absorbed), or miss the object and fly back out to the ambient plasma. If the plasma potential is taken to be zero, all of these ions have positive energy and cannot be confined near the object. However, Bernstein and Rabinowitz[11] commented in 1959 that if there are occasional collisions near the object, ions can lose energy and be unable to escape from the negative potential well. The density of these trapped ions can thus

[a)]Electronic mail: lampe@ppd.nrl.navy.mil

 

slowly build up until it reaches an appreciable level, which could play a very important role in the dynamics. Since they found the population of trapped ions to be ''determined by collisions and most difficult to calculate,'' Bernstein and Rabinowitz carefully specified that ''in order to obtain a tractable problem'' their calculation would be restricted to objects larger than a specified size, for which trapped ions cannot occur. Down through the years, a number of other authors commented that trapped ions could be important, but that the trapped ion problem would probably not be tractable.[2,11,17,18] Collisionless theories were thus generally used for dusty plasma, even though trapped ions should be important for the small dust grains.[18]

In 1992, Goree[17] made a most remarkable observation. He noted that once a trapped ion is created, it will orbit the grain and remain in the potential well until it has another collision which either kicks it out of the well, or causes it to fall onto the grain and be absorbed. Since the creation rate of trapped ions is proportional to the collision frequency $\nu$, and the loss rate is also proportional to $\nu$, the density of trapped ions must be *independent* of $\nu$ in steady state. Goree also confirmed in a Monte Carlo simulation that the total number of trapped ions can be quite significant. In 2000 Zobnin *et al.*[18] performed a more detailed Monte Carlo simulation, actually calculating the trapped ion density profile $n_t(r)$ and the self-consistent potential $\phi(r)$. They also found that $n_t(r)$ is indeed large.

In a recent Letter,[19] we sketched out a fully analytic method for calculating the distribution of trapped as well as untrapped ions, and solved self-consistently for $n_t(r)$, $\phi(r)$, and the untrapped ion density $n_u(r)$. We showed that under typical conditions the inner part of the shielding cloud is made up primarily of trapped ions, and that $\phi(r)$ is thus different from the results of the collisionless OML theory. In the present paper, we give the complete derivation of those results, and we calculate in addition the ion distribution function and the collisional ion current to the grain. We find that the collisional current is usually dominant, even in regimes of fairly low collisionality, because in steady state the trapped ion density is very large and essentially all trapped ions eventually fall onto the grain (after a sequence of collisions). Since collisionality substantially increases the ion current, the negative floating potential $\phi_f$ of the grain is reduced to as little as 50% of the widely used OML result. The grain charge is proportional to $\phi_f$, and thus can also be substantially smaller than the OML result.

The outline of the paper is as follows: In Sec. II, we introduce the model and its assumptions, and derive the equations that determine $n_t(r)$, $n_u(r)$, $\phi(r)$, and the ion distribution function $f_i(r,\mathbf{v})$. In Sec. III we derive the collisional contribution to the ion current, and show how to calculate $\phi_f$ fully self-consistently. In Sec. IV, we give the results for some specific cases, and discuss the general nature of the solutions. In Sec. V we summarize and discuss some future directions for research. In the Appendix we evaluate the validity of one of our key assumptions, the neglect of centrifugal potential barriers to the radial motion.

## II. SELF-CONSISTENT CALCULATION OF THE POTENTIAL AND THE TRAPPED ION DISTRIBUTION

### A. Model and assumptions

We consider a steady state consisting of a single stationary spherical grain of radius $a$, immersed in a plasma, with no magnetic field. The grain is assumed to be small compared to the Debye length $\lambda_D \equiv [4\pi n_0 e^2(T_e^{-1}+T^{-1})]^{-1/2}$. The plasma consists of positive ions, assumed for convenience to be singly-charged, electrons, and neutral molecules. In the ambient plasma, all species are assumed to be Maxwellian, with temperatures $T_e$ for electrons and $T$ for both ions and neutrals. (The calculation can easily be extended to the case where the ion and neutral temperatures are not equal.) We assume that none of the plasma species are flowing. The present calculation thus applies to dust grains in bulk plasma, e.g., grains that may be slowly settling through a discharge, or in a microgravity situation grains which permanently reside in the plasma. It should be noted that in typical dusty plasma laboratory experiments, the dust grains levitate at the edge of a sheath, where a strong electric field balances gravity. In this region, ions stream by the dust at a velocity of the order of the ion sound speed, and this ion flow has important consequences. The present calculation does not apply here, although we are looking into the possibility of extending it to this case.

We consider weakly-ionized discharges, where the dominant types of ion collision are normally charge-exchange and elastic collisions with neutrals. We include in our model only charge-exchange collisions, which we define as collisions that transfer an electron from the neutral to the ion, without any exchange of momentum. Thus a charge-exchange collision near the grain simply replaces a fast incoming ion with a slow ion whose velocity is chosen from the neutral molecule distribution. These collisions are particularly effective in creating trapped ions, or in causing a trapped ion to fall onto the grain. We shall neglect ion–ion collisions and elastic ion–neutral collisions.[20] We assume that the charge-exchange collision frequency $\nu$ is energy-independent.[21] This is an important simplification which enables us to develop an analytic model. Furthermore, we assume that $\nu$ is small, in the sense that the probability of a collision is small during the time for an untrapped ion to traverse the potential well, or for a trapped ion to make one rotation in its orbit. Roughly speaking, this is equivalent to the assumption that the mean free path $\lambda_{\rm mfp} \gg \lambda_D$.

Finally, we make an assumption that has been widely used as the basis of the orbital-motion-limited (OML) theory.[1–6,11–15] Our system is spherically symmetric about the grain, so (in between collisions) the energy $\epsilon$ and angular momentum $J$ of an ion are conserved. In spherical coordinates, the radial equation of motion for an ion can be written

$$m\ddot{r} = -U'(r), \tag{1}$$

where

$$U(r) \equiv e\phi(r) + \frac{J^2}{2mr^2} \tag{2}$$

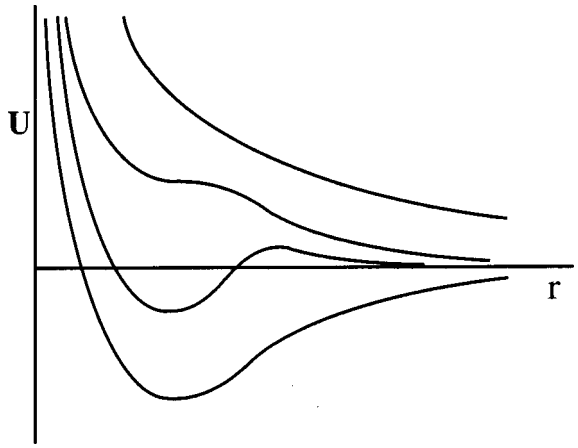


FIG. 1. Possible shapes for the radial effective potential $U(r)$.

is an effective potential energy for radial motion, including a centrifugal force term. The first term of (2) is attractive, while the centrifugal force term is repulsive. Depending on the value of $J$ and the details of $\phi(r)$, $U(r)$ can have no extrema, one minimum, or one minimum and one maximum, as shown in Fig. 1. Our assumption is that $U(r)$ has no maximum. It follows that, in the absence of a collision, the trajectory of an ion passes through all values of $r$ such that

$$e\phi(r)+\frac{J^2}{2mr^2}\leqslant\epsilon. \tag{3}$$

For positive-energy ions, this means all values of $r$ that lie between some $r_{\min}$ and $\infty$. Negative-energy ions, on the other hand, are trapped between some $r_{\min}$ and $r_{\max}$. The assumption that $U(r)$ has no maximum is not exactly correct for all ions.[5] However it has been shown[6] that it is a good approximation, because a maximum in $U(r)$ occurs only for ions in a small range of $J$, and the maximum is always so low that it blocks the trajectories of only a small number of ions. We shall elaborate further on this assumption in the Appendix.

### B. Distribution of ions created at a single location $r'$

Trapped ions are created by ion-neutral charge-exchange collisions. Every time a collision occurs, the old ion disappears, and a new ion is created whose velocity is chosen at random from the neutral molecule distribution function $\exp(-mv^2/2T)$. An ion from the ambient plasma is accelerated as it falls into the negative potential well surrounding the grain, so the result of a collision within the potential well is to replace a fast ion by a much slower ion, which probably cannot escape from the well. The new ion will either be lost promptly by falling onto the grain, or will become a trapped ion which orbits the grain. We begin our calculation by partitioning the trapped ion population into separate classes depending on the location where the previous collision occurred. Consider the class of trapped ions which were created by collisions at radial location $r'$, and let $h(r,v,\theta;r')$ be the phase-space distribution function of these ions. Here $r$ is the present location and $\mathbf{v}\equiv(v,\theta)$ is the present velocity of the ion; $\theta$ is the angle between $r$ and $v$. Because of spherical symmetry, $h(r,v,\theta;r')$ does not depend on the angular coordinates of $r$ and $r'$, nor on the azimuthal coordinate of $v$. If trapped ions were collisionless, then the steady-state Vlasov equation would tell us that the distribution function $h(r,v,\theta;r')$, for a given birthplace $r'$, is a function only of the constants of the motion, energy $\epsilon\equiv\frac{1}{2}mv^2+e\phi(r)$ and angular momentum $J\equiv mvr\sin\theta$. [Here we have used the assumption that $U(r)$ has no maxima, so that there are trajectories connecting all phase-space points that are accessible to an ion with specified $\epsilon$ and $\mathbf{J}$.] Since the ions are born Maxwellian, this distribution must be of the form,

$$h(r,v,\theta;r')=C(r')\exp\left(-\frac{mv^2}{2T}-\frac{e\phi(r)}{T}\right). \tag{4}$$

Actually, trapped ions do undergo charge-exchange collisions, and we do not want to neglect this. If a collision occurs at $r''$, the ion is lost from $h(r,v,\theta;r')$, and a new ion is added to a different class $h(r,v,\theta;r'')$. But we have assumed that the collision frequency $\nu$ is energy-independent, so there is no correlation between the value of $\mathbf{v}$ and the probability that a collision has occurred. Furthermore, we have assumed that the time between collisions $\nu^{-1}$ is long compared to the orbit period of a trapped ion. Thus there is essentially no correlation between the value of $r-r'$ and the probability that an ion created at $r'$ has had another collision before it gets to $r$. It follows that any ion in $h(r,v,\theta;r')$ is equally likely to have been lost to a collision. Therefore $h(r,v,\theta;r')$ must be of the form (4), even with collisions.

However, the Maxwellian distribution (4) is not populated by trapped ions for every value of $v$ and $\theta$. Several conditions must be satisfied. First, the ion must have negative total energy, i.e.,

$$\tfrac{1}{2}mv^2<-e\phi(r); \tag{5a}$$

otherwise it can escape to $r=\infty$ and is not a trapped ion. A second condition is that the total energy $\epsilon$ must be greater than $e\phi(r')$, since the ion was born at $r'$ with positive kinetic energy, i.e.,

$$e\phi(r')-e\phi(r)<\tfrac{1}{2}mv^2. \tag{5b}$$

A third condition is that the ion must have enough angular momentum so that its trajectory does not intercept the grain radius $a$. (Since we assume that the orbital period is short compared to the collision time, we treat ions whose trajectory intercepts the grain as if they are lost immediately, and just delete them from the trapped ion distribution.) Using conservation of energy and angular momentum, it is easy to show that if the ion is to miss the grain, it must have at least a minimum kinetic energy specified by

$$[e\phi(r)-e\phi(a)]\frac{a^2}{r^2-a^2}<\frac{1}{2}mv^2. \tag{5c}$$

If the ion does not satisfy (5c), it does not have enough energy to avoid falling onto the grain. But even if (5c) is satisfied, the ion must have enough perpendicular velocity to avoid falling onto the grain. Again using conservation of energy and angular momentum, this leads to a requirement on $\theta$,

$$\frac{a}{r}\sqrt{1+\frac{2[e\phi(r)-e\phi(a)]}{mv^2}}\equiv\sin\theta_0(r,v)<\sin\theta. \quad (5d)$$

Note that $0\leqslant\sin\theta_0\leqslant 1$ if (5c) is satisfied. We can combine (5a)–(5c) into a condition

$$v_0^2(r,r')<v^2<v_1^2(r), \quad (6)$$

where

$$\tfrac{1}{2}mv_1^2(r)\equiv -e\phi(r), \quad (7)$$

and $v_0(r,r')$ is the larger of the two minima specified by Eqs. (5b) and (5c). To summarize, Eq. (6) states that a trapped ion which was created at $r'$ but is now at $r$ must have (i) at least as much energy as it gained by falling from $r'$ to $r$; (ii) at least enough energy to avoid falling onto the grain; but (iii) not so much energy that it can escape from the potential well. It is also possible to show that if $r$ is small enough, condition (i) determines the minimum velocity $v_0$, but if $r$ is larger it is condition (ii) that is the controlling factor. Specifically,

$$\frac{1}{2}mv_0^2(r,r')\equiv\begin{cases}[e\phi(r')-e\phi(r)], & \text{if } r_0(r)\leqslant r',\\ [e\phi(r)-e\phi(a)]\dfrac{a^2}{r^2-a^2}, & \text{if } r'\leqslant r_0(r),\end{cases} \quad (8)$$

where $r_0$ is a function of $r$ defined as the solution of

$$\phi(r_0)=\frac{r^2\phi(r)-a^2\phi(a)}{r^2-a^2}. \quad (9)$$

We note that (6) can only be satisfied if $v_0^2(r,r')\leqslant v_1^2(r)$, which requires that

$$[e\phi(r)-e\phi(a)]\frac{a^2}{r^2-a^2}<-e\phi(r), \quad (10)$$

or equivalently

$$r^2\phi(r)<a^2\phi(a). \quad (11)$$

Equation (11) is easily satisfied for small grains ($a\ll\lambda_D$) and small values of $r\ll\lambda_D$, where $\phi(r)$ is roughly the bare Coulomb potential, and we recall that $\phi<0$. But for $r>\lambda_D$ shielding becomes strong, and eventually Eq. (11) fails for $r$ greater than some radius which we shall call $r_1$. Trapped ions cannot exist for $r>r_1$, because in this region the potential well is very shallow, and negative-energy ions cannot have enough angular momentum to escape falling onto the grain.[22] Thus there are no orbiting trapped ions if the grain size is very large, $a>r_1$.

Taking account of all of the constraints (6)–(11), we see that $h(r,v,\theta;r')$ is a function that is Maxwellian in $v$ and in $e\phi(r)$, but with many voids in phase space where $h(r,v,\theta;r')=0$. The presence of these voids can be made explicit by including appropriate step functions in the definition of $h(r,v,\theta;r')$, i.e., by rewriting Eq. (4) as

$$h(r,v,\theta;r')=C(r')\exp\left(-\frac{mv^2}{2T}-\frac{e\phi(r)}{T}\right)\times\Theta(r_1-r')\Theta(r_1-r)\Theta[v_1(r)-v]\times\Theta[v-v_0(r,r')]\Theta[\sin\theta-\sin\theta_0(r,v)], \quad (12)$$

where

$$\Theta(x)\equiv\begin{cases}1, & \text{if } x\geqslant 0,\\ 0, & \text{if } x\leqslant 0.\end{cases}$$

### C. Calculation of the coefficient $C(r')$

We can use the steady state condition to determine the coefficient $C(r')$. As a first step, we define a quantity $g(r')$ such that in steady state $4\pi r'^2 g(r')dr'$ is the total number of trapped ions which were born in the volume element between $r'$ and $r'+dr'$. $g(r')$ is thus the integral of $h(r,v,\theta;r')$ over $r$, $v$, and $\theta$,

$$\begin{aligned}g(r')&=C(r')\Theta(r_1-r')\int_a^{r_1}4\pi dr r^2 e^{-[e\phi(r)/T]}\times\int_{v_0(r,r')}^{v_1(r)}2\pi dv v^2 e^{-(mv^2/2T)}\int_{0_0(r,v)}^{\pi-\theta_0(r,v)}d\theta\sin\theta\\&\equiv 16\pi^2 C(r')\Theta(r_1-r')\int_a^{r_1}dr r^2 G(r,r'),\end{aligned} \quad (13)$$

where

$$\begin{aligned}G(r,r')&=\frac{1}{2}e^{-[e\phi(r)/T]}\int_{v_0(r,r')}^{v_1(r)}dv v^2 e^{-(mv^2/2T)}\times\int_{\theta_0(r,v)}^{\pi-\theta_0(r,v)}d\theta\sin\theta\\&=e^{-[e\phi(r)/T]}\int_{v_0(r,r')}^{v_1(r)}dv v^2 e^{-(mv^2/2T)}\times\sqrt{1-\frac{a^2}{r^2}-\frac{2a^2}{r^2}\frac{e\phi(r)-e\phi(a)}{mv^2}}\\&=\left(\frac{2T}{m}\right)^{3/2}\sqrt{\frac{r^2-a^2}{r^2}}\exp\left(\frac{-r^2e\phi(r)+a^2e\phi(a)}{(r^2-a^2)T}\right)\times\int_{u_0(r,r')}^{u_1(r)}du u^2 e^{-u^2}.\end{aligned} \quad (14)$$

In the last step of Eq. (14), the integral is reduced to an error function form by using the new variable,

$$u\equiv\sqrt{\frac{mv^2}{2T}-\frac{a^2}{r^2-a^2}\frac{e\phi(r)-e\phi(a)}{T}}, \quad (15)$$

and $u_0(r,r')$, $u_1(r)$ are given by Eq. (15) with $v_0(r,r')$, $v_1(r)$ substituted for $v$.

An ion is lost from $g(r')$ every time one of these ions has a collision, i.e., the loss rate is

$$\left[\frac{dg(r')}{dt}\right]_{\text{loss}} = -\nu g(r'). \tag{16}$$

In steady state, this loss rate must be equal to the rate at which ions are added to $g(r')$ by collisions at $r'$. The rate of collisions at $r'$ is simply $\nu[n_u(r')+n_t(r')]$, and each of these collisions creates a new ion. But the new ion is a trapped ion which contributes to $g(r')$ only if conditions (5d), (6), and (11) are satisfied, with $r'=r$. Thus the creation rate is

$$\begin{aligned}\left[\frac{dg(r')}{dt}\right]_{\text{creation}} &= \nu\Theta(r_1-r')[n_u(r')+n_t(r')] \\ &\quad\times\frac{\int_{v_0(r',r')}^{v_1(r')}dv v^2 e^{-(mv^2/2T)}\int_{\theta_0(r',v)}^{\pi-\theta_0(r',v)}d\theta\sin\theta}{\int_0^\infty dv v^2 e^{-(mv^2/2T)}\int_0^\pi d\theta\sin\theta} \\ &= 4\pi^{-1/2}\nu\left(\frac{2T}{m}\right)^{-3/2}\Theta(r_1-r') \\ &\quad\times[n_u(r')+n_t(r')]e^{[e\phi(r')/T]}G(r',r').\end{aligned} \tag{17}$$

Using Eqs. (13)–(17), we can solve for $C(r')$, giving

$$\begin{aligned}h(r,v,\theta;r') &= \frac{1}{4\pi^{5/2}}\left(\frac{2T}{m}\right)^{-(3/2)}[n_u(r')+n_t(r')]e^{-(mv^2/2T)} \\ &\quad\times e^{[e\phi(r')-c\phi(r)]/T}\frac{G(r',r')}{\int_a^{r_1}dr''r''^2G(r'',r')} \\ &\quad\times\Theta(r_1-r')\Theta(r_1-r)\Theta[v_1(r)-v] \\ &\quad\times\Theta[v-v_0(r,r')]\Theta[\sin\theta-\sin\theta_0(r,v)].\end{aligned} \tag{18}$$

### D. Calculation of the trapped ion density and the potential

We can now calculate the trapped ion density $n_t(r)$ by integrating $h(r,v,\theta;r')$ over $(v,\theta;r')$. Since $n_t(r')$ also appears as a source term on the RHS of Eq. (18), this procedure actually yields a linear integral equation for $n_t(r)$,

$$n_t(r) = \int_a^{r_1}dr'K(r,r')n_t(r') + \int_a^{r_1}dr'K(r,r')n_u(r'), \tag{19}$$

where

$$\begin{aligned}K(r,r') &= \frac{4}{\pi^{1/2}}\left(\frac{2T}{m}\right)^{-3/2} \\ &\quad\times\frac{r'^2e^{[e\phi(r')/T]}G(r',r')G(r,r')}{\int_a^{r_1}dr''r''^2G(r'',r')}\Theta(r_1-r).\end{aligned} \tag{20}$$

To complete the calculation, it is necessary to solve Eq. (19) self-consistently with Poisson's equation,

$$\frac{1}{r^2}\frac{d}{dr}r^2\frac{d\phi}{dr} = 4\pi e[n_u(r)+n_t(r)-n_e(r)]. \tag{21}$$

In Eq. (21), the trapped ion density is determined from the self-consistent solution of (19). The electron density $n_e(r)$ can be accurately approximated by a Boltzmann factor,[14]

$$n_e(r) = n_0\exp[e\phi(r)/T_e]. \tag{22}$$

The untrapped ion density $n_u(r)$ is specified as an explicit functional of $\phi(r)$ by the OML theory,[4]

$$\begin{aligned}\frac{n_u(r)}{n_0} &= \frac{2}{\sqrt{\pi}}\exp\left(-\frac{e\phi(r)}{T}\right)\int_{\sqrt{-e\phi(r)/T}}^\infty dt t^2e^{-t^2} \\ &\quad\times\left[1+\sqrt{1-\frac{a^2}{r^2}\left(1+\frac{e[\phi(r)-\phi(a)]}{Tt^2}\right)}\right] \\ &= \frac{2}{\sqrt{\pi}}e^{-e\phi(r)/T}\int_{\sqrt{-e\phi(r)/T}}^\infty dt t^2e^{-t^2} \\ &\quad+\frac{2}{\sqrt{\pi}}\sqrt{\frac{r^2-a^2}{r^2}}\exp\left(\frac{-r^2e\phi(r)+a^2e\phi(a)}{(r^2-a^2)T}\right) \\ &\quad\times\int_{\sqrt{[-r^2e\phi(r)+a^2e\phi(a)]/(r^2-a^2)T}}^\infty dt t^2e^{-t^2},\end{aligned} \tag{23}$$

where the first integral is taken only over values of $t$ such that the argument of the square root is positive.

Finally, it is necessary to specify boundary conditions for Eq. (21) at $r=a$ and $r=\infty$. The boundary condition is at $r=\infty$ is of course $\phi(\infty)=0$. The boundary condition at $r=a$ depends on the physical situation. If the collector is a probe biased to a specified potential $\phi_0$, the boundary condition is simply $\phi(a)=\phi_0$. If the collector is a dust grain, $\phi(a)$ is set equal to the floating potential $\phi_f$, i.e., the potential for which the electron flux $F_e$ to the grain is equal to the ion flux $F_i$,

$$F_e = F_i. \tag{24}$$

Taking a velocity moment over the Maxwell–Boltzmann distribution, the electron flux is found to be

$$F_e = n_0\sqrt{\frac{T_e}{2\pi m_e}}e^{e\phi_f/T_e}. \tag{25}$$

In the limit $\nu\to 0$, $F_i$ is entirely due to untrapped ions, and the ion flux is given by OML theory,[8]

$$F_{\text{OML}} = n_0\sqrt{\frac{T}{2\pi m}}\left(-\frac{e\phi_f}{T}+1\right). \tag{26}$$

Using (25) and (26) in (24), we obtain the well-known OML result that $\phi_f$ is the solution of

$$\left(1-\frac{e\phi_f}{T}\right)\exp\left(-\frac{e\phi_f}{T_e}\right) = \left(\frac{mT_e}{m_eT}\right)^{1/2}. \tag{27}$$

Typically Eq. (27) gives $e\phi_f\approx -T_e$ to $-3T_e$, depending on the ion mass. However, we shall see that for finite values of

$\nu$, $F_i$ is usually dominated by trapped ions, and is often substantially larger than $F_{\mathrm{OML}}$ from (26). Thus it is necessary to evaluate $F_i$ from the trapped ion distribution and solve (24) numerically for $\phi_f$. This will be discussed in Sec. III below.

### E. Solution procedure

A procedure for solving Eqs. (19)–(27) is as follows:

(i) Rewrite Poisson's equation, together with the boundary condition $\phi(\infty)=0$, in the form of Gauss' law,

$$\phi(r)=-Ze\left[\frac{1}{r}+\int_r^\infty \frac{dr'[Q_t(r)+Q_u(r)+Q_e(r)]}{r'^2}\right], \tag{28}$$

where $-Ze$ is the grain charge, $ZeQ_t(r)$ is the trapped ion charge contained within radius $r$, $ZeQ_u(r)$ is the deviation of the untrapped ion charge contained within radius $r$ from the ambient value $(4\pi/3)r^3n_0e$, and $ZeQ_e(r)$ is the deviation of the electron charge within radius $r$ from the ambient value.

(ii) Begin with the OML solution[4] for $\phi(r)$ and $n_u(r)$, i.e., the solution of Eqs. (21)–(23), with boundary condition (27). This includes no trapped ions. Call these $\phi^{(0)}(r)$ and $n_u^{(0)}(r)$. Use $\phi^{(0)}(r)$ in Eqs. (14) and (20) to evaluate $K(r,r')$.

(iii) Calculate a first approximation $n_t^{(1)}(r)$ to the trapped ion density from Eq. (19), neglecting the first term on the RHS. $n_t^{(1)}(r)$ can be interpreted as the population of ''first generation'' trapped ions created by collisions of untrapped ions. Integrate $n_t^{(1)}(r)$ to obtain $Q_t^{(1)}(r)$.

(iv) Recalculate $\phi(r)$ from Eq. (28), choosing $Z$ so that the boundary condition (24) is satisfied. In the limit of small $\nu$, this just means $\phi_f$ must satisfy (27). For finite $\nu$, it is necessary to explicitly calculate the electron and ion flux to the grain and choose $Z$ so that they are equal. This will be discussed in Sec. III. Using the new $\phi^{(1)}(r)$, recalculate $G(r,r')$, $K(r,r')$, $n_u(r)$, and $n_e(r)$ from Eqs. (14), (20), (22), (23).

(v) Calculate a second iterate $n_t^{(2)}(r)$ by using $n_t^{(1)}(r)$ in the first term on the RHS of (19). $n_t^{(2)}(r)$ can be regarded as the population of trapped ions created by either the collision of an untrapped ion, or of a first-generation trapped ion.

(vi) Go back to step (iv) and proceed with this iteration scheme to convergence. To prevent overshoots in the iteration process, it is sometimes useful to subdivide the iteration [adding in only a fraction of the correction to $n_t(r)$ at each iteration step], but in practice the solution converges after only a few iterations.

In Sec. IV, results will be shown in a variety of cases for $n_t(r)$, $n_u(r)$, $\phi(r)$, and for the ion flux $F_i$ and the grain potential $\phi_f$ as a function of collision frequency $\nu$.

### F. Distribution function of trapped ions

After solving for $\phi(r)$, we can write down an explicit expression for the trapped ion distribution function $f_t(r,v,\theta)$ by integrating $h(r,v,\theta;r')$ over the source location $r'$. Taking account of all of the step functions in Eq. (18) for $f_t(r,v,\theta)$, and both requirements on $v_0(r,r')$ from (8), this gives

$$\begin{aligned} f_t(r,v,\theta)=&\Theta(r_1-r)\Theta[v_1(r)-v] \\ &\times\Theta\left[\frac{1}{2}mv^2-\frac{a^2[e\phi(r)-e\phi(a)]}{r^2-a^2}\right] \\ &\times\Theta[\sin\theta-\sin\theta_0(r,v)]\left(\frac{m}{2\pi T}\right)^{3/2}e^{-(mv^2/2T)} \\ &\times\int_a^{r_1}dr'r'^2\Theta\left[\frac{1}{2}mv^2+e\phi(r)-e\phi(r')\right] \\ &\times\frac{[n_u(r')+n_t(r')]G(r',r')}{\int_a^{r_1}dr''r''^2G(r'',r')}e^{[e\phi(r')-e\phi(r)]/T}. \end{aligned} \tag{29}$$

The results for $f_t(r,v,\theta)$ will be shown in Sec. IV.

## III. COLLISIONAL CONTRIBUTION TO THE ION CURRENT

Equation (26) from OML theory gives the ''collisionless'' flux of untrapped ions to the grain, $F_{\mathrm{OML}}$. More precisely, OML theory assumes that the mean free path is so large that essentially all collisions occur far from the grain, where the potential is zero. It is further assumed that the ion distribution is Maxwellian in the ambient plasma, i.e., at sufficiently large $r$. As Bernstein and Rabonowitz[11] pointed out, there must be collisions which maintain the Maxwellian distribution, but it is not necessary in OML theory to take these collisions explicitly into account, since the ions which deposit on the grain are assumed to come in from the Maxwellian ambient plasma without having any additional collisions.

In reality an ion may have a charge-exchange collision near the grain, on its way in from the ambient plasma. If a charge-exchange collision occurs, the energy of the newly created ion is on average less than that of the ion that it replaces, and therefore the new ion is statistically more likely to fall onto the grain. Thus collisions increase the ion flux to the grain. It is easy to see that this increase can be very substantial, even when the mean free path is quite large. To estimate the collisional effect, it is useful to think of the radius $r_T$, such that $e\phi(r_T)=-3T/2$, as the outer edge of the sheath around the grain. Normally, $r_T$ is in the vicinity of $\lambda_D$ to $2\lambda_D$. If an incoming untrapped ion undergoes a collision within $r<r_T$, a fast ion (which probably would not have hit the grain) is removed, and a slow ion is created which probably cannot escape from the potential well. This ion may fall onto the grain immediately if it happens to have low angular momentum. If the ion has enough angular momentum, it will orbit the grain rather than contacting it, but eventually will have another charge-exchange collision. On average, each collision brings the ion to a lower-energy state closer to the grain, and eventually the resulting ion will fall onto the grain. Thus, essentially every collision of an untrapped ion within $r<r_T$ results in an ion depositing on the grain. The collection area of the sheath is $\pi r_T^2$, which is very large compared to the cross-section $\pi a^2$ of the grain. How-

ever this area must be weighted by the probability that an ion–neutral charge-exchange collision occurs while the ion is in the sheath. Roughly speaking this probability is of order $r_T/\lambda_{\rm mfp}$, where $\lambda_{\rm mfp}$ is some average mean free path. Thus the ion flux to the grain, due to charge-exchange collisions at $r<r_T$, is

$$F_{\rm coll}\approx \frac{r_T^3}{a^2\lambda_{\rm mfp}}F_{\rm th}, \tag{30}$$

where $F_{\rm th}$ is the thermal flux in the ambient plasma, $F_{\rm th}=n_0(T/2\pi m_i)^{1/2}$. This should be added to the OML flux, to obtain an approximate expression for ion flux to the grain that is accurate to first order in $r_T/\lambda_{\rm mfp}$,

$$F_i\approx\left(1-\frac{e\phi_f}{T}+\frac{r_T^3}{a^2\lambda_{\rm mfp}}\right)F_{\rm th} \tag{31}$$

for ions of energy $T$. An approximate version of this expression (not including the effect of shielding) was given by Natanson[23] in 1960. For dusty plasmas with a $\ll\lambda_D$, the collisional contribution (30) is usually larger. It should be noted that Eq. (30) is actually an underestimate of the collisional deposition, because a collision which occurs on the fringes of the potential well at $r>r_T$ also slightly increases the probability that the ion will deposit on the grain. The cumulative effect of these distant collisions (over a large volume) also contributes to the collisional deposition.

We shall now calculate the ion flux $F_i$ to the grain. Our calculation includes both the OML flux and the "collisional" flux in a unified way; we shall show explicitly that the OML flux is the result of collisions within the ambient plasma, while the "collisional" flux is the result of collisions within the potential well around the grain. Assuming that the plasma dimensions are large compared to the mean free path, any ion that reaches the grain will have had a collision at some time in its past. Let $r'$ be the place at which the last collision occurred. We can write $F_i$ as an integral over the rate at which collisions occur at point $r'$, multiplied by the probability $p(r')$ that the new ion created by a collision at $r'$ will deposit on the grain without having another collision,

$$F_i=\frac{\nu}{4\pi a^2}\int_a^\infty dr' 4\pi r'^2[n_t(r')+n_u(r')]p(r'). \tag{32}$$

To calculate $p(r')$, let us first consider an ion created at $r'$ with velocity $v$, on a trajectory that will intersect the grain. The probability that this ion will reach the grain without having another collision is

$$P_{\rm coll}(r',\mathbf{v})=\exp\left[-\nu\int_a^{r'}dr/|v_r(r)|\right], \tag{33a}$$

where $v_r(r)$ is the ion's radial velocity when it is at position $r$. Exact evaluation of $P_{\rm coll}(r',v)$ would require numerical calculation of all of the phase space trajectories, but fortunately a simple and accurate approximation is possible. $P_{\rm coll}(r',\mathbf{v})$ plays an important role at large $r'$ ($r'>\lambda_{\rm mfp}$), where it prevents a divergence due to multiple counting of ions which undergo many collisions in the large volume outside the potential well. But $P_{\rm coll}(r',\mathbf{v})$ is close to unity for collisions within the potential well, $r'<r_T$, since the plasma has been assumed to be weakly collisional, i.e., $r_T\sim\lambda_D\ll\lambda_{\rm mfp}$. Thus it is sufficient to write an approximate expression for $P_{\rm coll}(r',\mathbf{v})$ which becomes exact in the large-$r'$ limit, and goes to unity at $r'\ll\lambda_{\rm mfp}$. To do this, we note that an ion that starts at $r'>\lambda_{\rm mfp}$, and whose trajectory intersects the grain without a collision, will necessarily follow a trajectory that is nearly radial.[24] The length of the trajectory will thus be close to $r'-a$, and in fact it is good enough to approximate it as $r'$. Furthermore, almost all of the time on the trajectory will be spent at $r'>r_T$, where $v$ is close to its initial value. Thus it is sufficiently accurate to approximate the (energy-dependent) mean free path as $\lambda_{\rm mfp}\approx v/\nu$. We can then write

$$P_{\rm coll}(r',\mathbf{v})=e^{-\nu r'/v}. \tag{33b}$$

Next, we note that, according to Eqs. (5c) and (5d), an ion's trajectory will intersect the grain if it satisfies any of the following four conditions:

(a) Incoming ions with low initial kinetic energy:

$$\frac{mv^2}{2}\leqslant\frac{a^2}{r'^2-a^2}[e\phi(r')-e\phi(a)],\quad \frac{\pi}{2}\leqslant\theta_0\leqslant\pi. \tag{34a}$$

(b) Incoming ions with higher kinetic energy but low angular momentum:

$$\frac{a^2}{r'^2-a^2}[e\phi(r')-e\phi(a)]\leqslant\frac{mv^2}{2},\quad \pi-\theta_0\leqslant\theta\leqslant\pi. \tag{34b}$$

(c) Outgoing *trapped* ions with low initial kinetic energy:

$$\frac{mv^2}{2}\leqslant\frac{a^2}{r'^2-a^2}[e\phi(r')-e\phi(a)],$$
$$\frac{mv^2}{2}\leqslant-e\phi(r'),\quad 0\leqslant\theta\leqslant\frac{\pi}{2}. \tag{34c}$$

(d) Outgoing *trapped* ions with higher kinetic energy but low angular momentum:

$$\frac{a^2}{r'^2-a^2}[e\phi(r')-e\phi(a)]\leqslant\frac{mv^2}{2}\leqslant-e\phi(r'),$$
$$\theta\leqslant\theta_0. \tag{34d}$$

In Eq. (34), $\theta_0$ is given by Eq. (5d). The probability $p(r')$ is thus given by

$$p(r')=\frac{\int\int_A dv v^2 d\theta\sin\theta\exp\left(-\frac{mv^2}{2T}-\frac{\nu r'}{v}\right)}{\int_0^\infty dv v^2 e^{-mv^2/2T}\int_0^\pi d\theta\sin\theta}, \tag{35}$$

where $A$ is the area of $v-\theta$ space which satisfies conditions (34). After doing the $\theta$-integral and collecting terms, the double integral in Eq. (35) becomes

$$p(r')=\frac{2}{\sqrt{\pi}}\int_0^\infty duu^2\exp\left(-u^2-\frac{\nu r'}{v_{\rm th}u}\right)+\frac{2}{\sqrt{\pi}}\int_0^{\sqrt{-e\phi(r')/T}}duu^2\exp\left(-u^2-\frac{\nu r'}{v_{\rm th}u}\right)$$
$$-\frac{2}{\sqrt{\pi}}\sqrt{\frac{r'^2-a^2}{r'^2}}\int_{\sqrt{a^2[e\phi(r')-e\phi(a)]/(r'^2-a^2)T}}^\infty duu\exp\left(-u^2-\frac{\nu r'}{v_{\rm th}u}\right)\sqrt{u^2-\frac{a^2[e\phi(r')-e\phi(a)]}{(r'^2-a^2)T}}$$
$$-\frac{2}{\sqrt{\pi}}\Theta[a^2\phi(a)-r'^2\phi(r')]\sqrt{\frac{r'^2-a^2}{r'^2}}\int_{\sqrt{\{a^2[e\phi(r')-e\phi(a)]/(r'^2-a^2)T}}^{\sqrt{[e\phi(r')/T]}}duu$$
$$\times\exp\left(-u^2-\frac{\nu r'}{v_{\rm th}u}\right)\sqrt{u^2-\frac{a^2[e\phi(r')-e\phi(a)]}{(r'^2-a^2)T}},\tag{36}$$

where $v_{\rm th}\equiv(2T/m)^{1/2}$.

Equations (32) and (36) specify the ion current to the grain. Results will be shown in Sec. IV. We find that for typical small but finite values of $\nu$, the dominant contribution to Eq. (32) is from collisions that occur within the potential well, at $r'<r_T$, and that $F_i$ is larger than $F_{\rm OML}$. This is because the density of trapped ions is very large near the grain, and a charge-exchange collision near the grain is very likely to yield an ion that falls immediately onto the grain. Thus, for realistic values of $\nu$ it is necessary to calculate the floating potential $\phi_f$ by setting $F_i$ from (32), (36) equal to $F_e$ from (25). Since the ion current is substantially larger than the OML value, the floating potential $\phi_f$ is significantly reduced as compared to the OML result (27).

However, Eqs. (32) and (36) also reduce to the usual OML result in the limit $\nu\to0$. In this limit, the dominant contribution to the integral in (32) is from collisions that occur in the range $r'>v_{\rm th}/\nu$, i.e., one or more mean free paths away from the grain. Let us separate the integral into a range from $a$ to $s$, and a range from $s$ to $\infty$, where $s$ is some point such that

$$r_T\ll s\ll v_{\rm th}/\nu,\tag{37a}$$
$$e|\phi(s)|\ll T,\tag{37b}$$
$$\frac{a^2|\phi(a)|}{s^2T}\ll1.\tag{37c}$$

Clearly, in Eq. (32) the contribution to $F_i$ from the range from $a<r'<s$ vanishes as $\nu\to0$, and thus in this limit

$$F_i=\frac{\nu}{4\pi a^2}\int_s^\infty dr4\pi r'^2[n_t(r')+n_u(r')]p(r').\tag{38}$$

The inequalities (37) are satisfied for all $r>s$. Expanding Eq. (36) in all of the small parameters, and additionally using the fact[11,15,4] that $\phi(r)\propto r^{-2}$ as $r\to\infty$, we find that to lowest order

$$p(r')=\frac{a^2}{\sqrt{\pi}r^2}\int_0^\infty duu^2\exp\left(-u^2-\frac{\nu r'}{v_{\rm th}u}\right)$$
$$-\frac{a^2e\phi(a)}{\sqrt{\pi}r^2T}\int_0^\infty du\exp\left(-u^2-\frac{\nu r'}{v_{\rm th}u}\right).\tag{39}$$

Inserting (39) in (32), reversing the order of integration, and using $n(r')\approx n_0$ for $r\gg r_T$, we find

$$F_i\approx\frac{\nu n_0a^2}{\sqrt{\pi}}\int_0^\infty du\left[u^2-\frac{e\phi(a)}{T}\right]e^{-u^2}\int_s^\infty dr'\exp\left(-\frac{\nu r'}{v_{\rm th}u}\right)$$
$$=\frac{n_0a^2v_{\rm th}}{\sqrt{\pi}}\int_0^\infty duu\left[u^2-\frac{e\phi(a)}{T}\right]e^{-u^2}\exp\left(-\frac{\nu s}{v_{\rm th}u}\right)$$
$$\approx\frac{n_0a^2v_{\rm th}}{\sqrt{\pi}}\int_0^\infty duu\left[u^2-\frac{e\phi(a)}{T}\right]e^{-u^2}$$
$$=n_0\sqrt{\frac{T}{2\pi m}}\left[1-\frac{e\phi(a)}{T}\right],\tag{40}$$

which is the OML flux. Notice that the coefficient $\nu$ canceled out of Eq. (38), because the integral in (38) is itself proportional to $\nu^{-1}$ as $\nu\to0$. The lower bound $s$ of the integral, which was chosen somewhat arbitrarily, also drops out to lowest order. In essence, the OML flux arises from collisions that occur in a region of the plasma where $\phi(r')=0$, i.e., where the presence of the grain has no influence. Our work extends the theory to first order in $\nu$ by including collisions which occur near the grain, where $\phi(r')\neq0$, but still requiring that $\lambda_D\ll\lambda_{\rm mfp}$.

## IV. RESULTS AND DISCUSSION

### A. Nearly collisionless limit

The theory developed in Secs. II and III depends on three dimensionless parameters, $T/T_e$, $a/\lambda_D$, and a measure of the collisionality which we choose to be $\nu\lambda_D/v_{\rm th}$. (Note that we have assumed that $\nu$ is constant, and therefore the mean free path $v/\nu$ is proportional to $v$. The ratio of $\lambda_D$ to the mean free path is thus of order $\nu\lambda_D/v_{\rm th}$ in the ambient plasma, but within the potential well the ion velocities are much larger, and thus the mean free path is much larger. Thus $\nu\lambda_D/v_{\rm th}$ is actually an overestimate of the collisionality of the plasma.) We shall present solutions for a variety of parameter choices, listed in Table I.

We consider first the situation in the limit of very small (but nonzero) $\nu\lambda_D/v_{\rm th}$. Then the ion current is given by $F_{\rm OML}$ of Eq. (26), the floating potential is given by Eq. (27),

TABLE I. Parameters for the numerical solutions. For Case 1, the exact value of $\nu\lambda_D/v_{\rm th}$ does not matter in Figs. 2–7, as long as it is small, but for Figs. 10–12 we use the explicit value $5\times10^{-5}$.

| Case number | Figure numbers | $T/T_e$ | $a/\lambda_D$ | $\nu\lambda_D/v_{\rm th}$ |
|---|---|---|---|---|
| 1 | 2–7 | 0.01 | 0.015 | $\rightarrow 0$ |
| 1 | 10–12 | 0.01 | 0.015 | $5\times10^{-5}$ |
| 2 | 6,7 | 0.01 | 0.1 | $\rightarrow 0$ |
| 3 | 6,7 | 0.04 | 0.015 | $\rightarrow 0$ |
| 4 | 10–12 | 0.01 | 0.015 | 0.037 |
| 5 | 10–12 | 0.01 | 0.015 | 0.47 |

and $n_t(r)$ and $\phi(r)$ are given by the self-consistent solution of Eqs. (19)–(23). The solution for a floating dust grain, for Case 1: $\nu\rightarrow 0$ and

$$T/T_e=0.01, \quad a/\lambda_D=0.015, \tag{41}$$

is shown in Figs. 2–5. Figure 2 shows the density $n_t(r)$ of trapped ions (solid curve); the deviation of the untrapped ion density from the ambient value, $\Delta n_u(r)\equiv n_u(r)-n_0$ (dashed curve); and the negative of the deviation from the ambient electron density, $-\Delta n_e(r)\equiv n_0-n_e(r)$ (dotted–dashed curve). Notice that $n_t\gg\Delta n_u\gg|\Delta n_e|$ near the grain, i.e., trapped ions dominate the shielding near the charged grain. In Fig. 3 we show the integrated charge densities $Q_t(r)$, $Q_u(r)$, and $Q_e(r)$, respectively the integrals of $en_t(r)$, $e\Delta n_u(r)$, and $-e\Delta n_e(r)$ from $a$ to $r$, each scaled to the grain charge $Ze$. Note that at $r=2\lambda_D$, the grain charge is 68% neutralized, with 41% due to trapped ions, 27% due to untrapped ions, and $<1\%$ due to electrons. At $r\rightarrow\infty$, 47% of the shielding is due to trapped ions, 52% to untrapped ions, and $<1\%$ to electrons. In Fig. 4, we plot $r\phi(r)$. On this semilog plot, the unshielded Coulomb potential would appear as a horizontal straight line, and the Debye-shielded potential would appear as the oblique dotted line. We plot the complete solution as the solid curve, and the OML solution (with no trapped ions) as the dashed curve. Note that the inclusion of the trapped ions increases the shielding and brings the potential to within 25% of the Debye-shielded potential for $r<5\lambda_D$. For large $r$, $\phi(r)$ is proportional to $r^{-2}$, as has been discussed previously.[11,15,4]

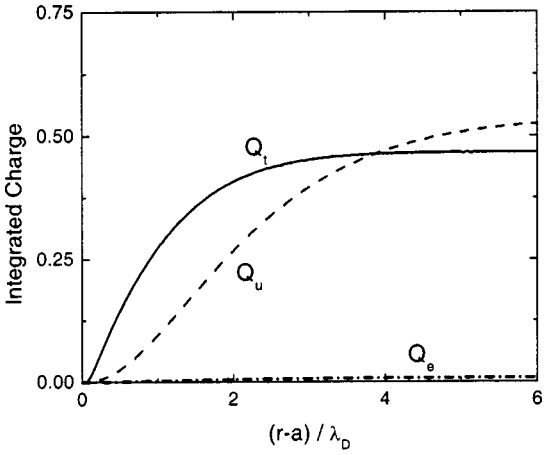


FIG. 3. Integrated trapped ion charge from $r=a$ to $r$ [$Q_t(r)$, solid], deviation of the integrated untrapped ion charge from ambient [$Q_u(r)$, dashed], and deviation of the integrated electron charge from ambient [$Q_e(r)$, dotted–dashed], all scaled to the charge on the grain, for Case 1.

In Fig. 5, we show ion distribution functions at three locations, (5a) $r=2a$, close to the grain; (5b) $r=10a$, midway in the sheath; (5c) $r=\lambda_D=66.6a$, close to the outer limit of the sheath. The distribution function consists of trapped ions for $\frac{1}{2}mv^2(r)<-e\phi(r)$ (negative total energy) and untrapped ions for $\frac{1}{2}mv^2(r)>-e\phi(r)$ (positive total energy). Both the trapped and untrapped portions of the distribution function $f_i(r,v,\theta)$ are isotropic functions $f(r,v)$, except that there are voids for certain ranges of $\theta$, representing ions whose trajectories intersect the grain. In Fig. 5 we have plotted the isotropic function $f(r,v)$ as a solid curve in the trapped ion region, and as a dashed curve in the untrapped ion region. These curves are on an arbitrary scale. We have also plotted the critical angle $\theta_0(r,v)$ which defines the voids, as will be explained below. This is the dotted curve, and it is on the scale shown at the left of the figure. We note

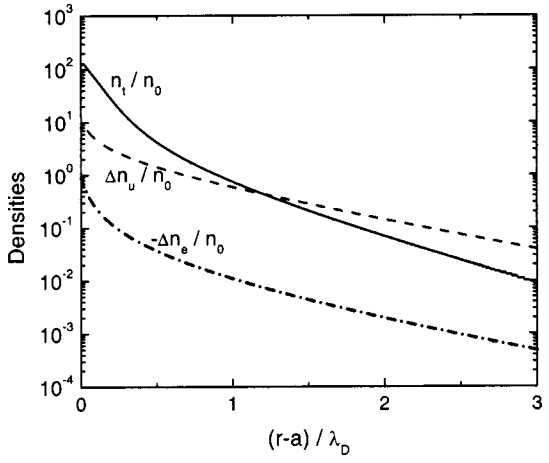


FIG. 2. Trapped ion density [$n_t(r)$, solid], deviation of untrapped ion density from ambient [$\Delta n_u(r)$, dashed], and deviation of electron density from ambient [$-\Delta n_e(r)$, dotted–dashed], all scaled to ambient density $n_0$, for Case 1: $T/T_e=0.01$, $a/\lambda_D=0.015$, $\nu\rightarrow 0$.

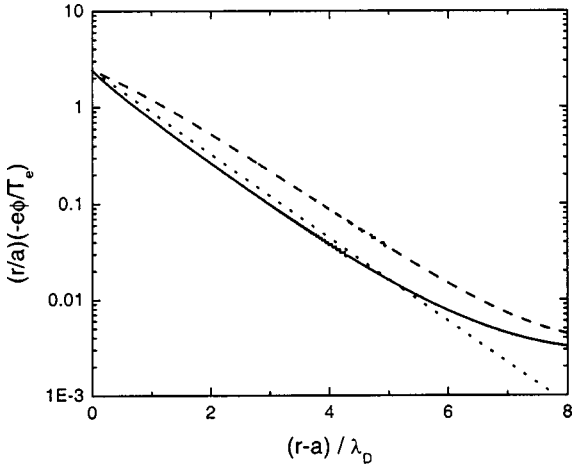


FIG. 4. Plot of $-(r/a)e\phi(r)/T_e$ for Case 1: self-consistent potential including trapped ions (solid), potential with trapped ions neglected (dashed), Debye potential (dotted).

that in all cases there is a discontinuity in $f(r,v)$ at the zero-energy point $\frac{1}{2}mv^2(r) = -e\phi(r)$, and that the nature of the distribution is very different for the trapped and untrapped ions.

Consider first the untrapped ions. Since the ambient ion distribution is Maxwellian, Liouville's equation indicates[4] that the untrapped part of the ion distribution at location $r$ is also a Maxwellian

$$f(r,v) = \text{const} \times \exp\left( -\frac{mv^2}{2T} - \frac{e\phi(r)}{T} \right),$$

except that outgoing ions whose trajectories have already intersected the grain are removed from the distribution. This forms a void in the Maxwellian for $\theta < \theta_0(r,v)$, where $\theta_0(r,v)$ is a monotonically decreasing function of both $r$ and $v$ which is defined by Eq. (5d).

For $\frac{1}{2}mv^2(r) < -e\phi(r)$ we have the trapped ion part of the distribution, given by Eq. (29). Outgoing ions whose trajectories have already intersected the grain are removed from the trapped ion distribution; hence there is a void for $\theta < \theta_0(r,v)$. But in addition, incoming ions whose trajectories will intersect the grain are removed from the trapped ion distribution. As explained in Sec. II B, this is done because these ions have a very short lifetime as compared to the orbiting trapped ions. Thus, for negative-energy ions, there is also a void in the distribution for $\pi - \theta < \theta_0(r,v)$. Note that $f(r,v)$ has a spike for trapped ions with slightly negative total energy. There are many such ions because they can be created by collisions that occur anywhere in the large volume at the edge of the potential well, where $\phi(r)$ is slightly negative. Smaller velocities in Fig. 5 correspond to more strongly trapped ions, which are created by collisions deeper within the sheath. The volume available for these collisions is smaller, but on the other hand there are many collisions at small $r$ because the ion density there is large (see Fig. 2). As a result of the balance between these opposing trends, $f(r,v)$ generally decreases at small values of $v$, but there is a gentle peak at moderate values of $v$ for the cases $r = 2a$ and $r = 10a$. Notice also that for very small $v$, $\theta_0(r,v)$ becomes larger than $\pi/2$. This means that the void has eaten up the entire distribution, and there are no trapped ions at all with these small values of $v$. The condition for this is that inequality (5c) is violated.

The results shown in Figs. 2–5 appear to present a paradox: we have assumed that the collision frequency $\nu$ is vanishingly small, and yet trapped ions, created only by collisions, are a dominant feature of the solution. Indeed, $\phi(r)$, $n_t(r)$, and $f_i(r,v,\theta)$ do not depend on the value of $\nu$, in this limit of small $\nu$. How can this be possible, since there are no trapped ions if $\nu = 0$? The explanation of the $\nu \to 0$ limit is that for any small but nonzero value of $\nu$ the creation rate of trapped ions is proportional to $\nu$ and the loss rate is also proportional to $\nu$, so the steady state is independent of $\nu$. However, the time necessary to reach steady state is inversely proportional to $\nu$, so steady state is never reached for $\nu = 0$. In practice, $\nu$ is always very fast compared to macroscopic times such as the lifetime of the discharge, or times characterizing the motion of a dust grain, so a steady state treatment is indeed appropriate.

Trapped ions clearly are a dominant player in the shielding around the grain, for Case 1. One may ask more generally under what conditions the density of trapped ions is large? The essential requirement is that nearly all of the new ions created by charge-exchange collisions within the sheath become trapped ions. There are two conditions for this: that the new ion does not escape to $r \to \infty$, nor does it fall onto the grain. The potential $\phi_f$ at the grain is of the order of $T_e$, while new ions are born with energy of the order of $T$. Thus, very few of the new ions can escape from the well, if $T/T_e \ll 1$. Provided this is true, the sheath can be regarded as extending roughly to the point $r_T$ (typically about $\lambda_D$ to $2\lambda_D$) where $e\phi(r_T) = -3T/2$. Equations (34) specify the conditions under which the new ion created at a point $r < r_T$ will fall onto the grain. These equations indicate that this is unlikely to happen if $a^2/r_T^2 \ll T/T_e$. When both of these conditions are satisfied,

$$a^2/r_T^2 \ll T/T_e \ll 1, \tag{42}$$

the steady state trapped ion population within the potential well greatly exceeds the untrapped ion population, since

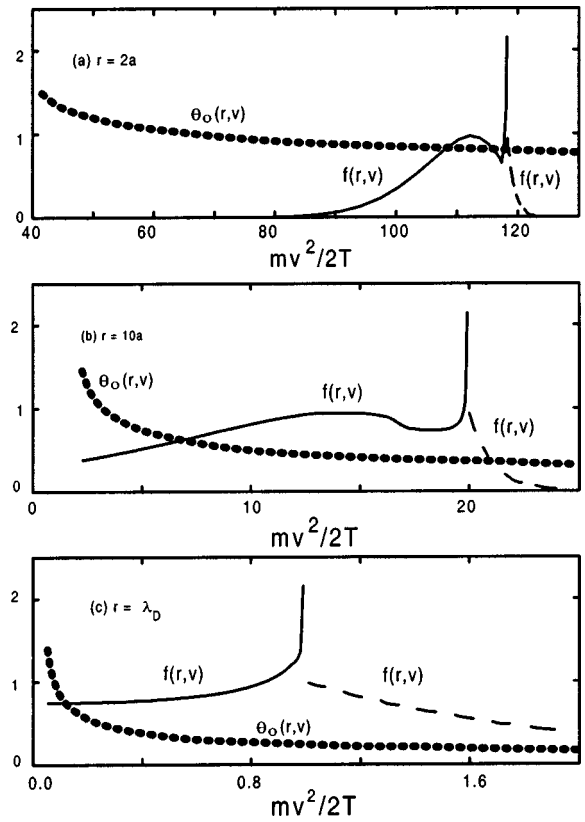


FIG. 5. The ion distribution function $f(r,v,\theta)$ is an isotropic function $f(r,v)$ which has voids for certain ranges of $\theta$, as discussed in the text. We show $f(r,v)$ for Case 1 at (a) $r = 2a$, (b) $r = 10a$, (c) $r = \lambda_D = 66.6a$. $f(r,v)$ is shown as a solid curve for the range $mv^2/2 < -e\phi(r)$ (trapped ions), and as a dashed curve for $mv^2/2 > -e\phi(r)$ (untrapped ions). These curves are on arbitrary scale. The quantity $\theta_0(r,v)$ which characterizes the voids in the distribution is shown as the dotted curves, with scale at left. For $v$ less than a critical value defined by Eq. (5c), $\theta_0(r,v) \geqslant \pi/2$, which means the distribution function is entirely void.

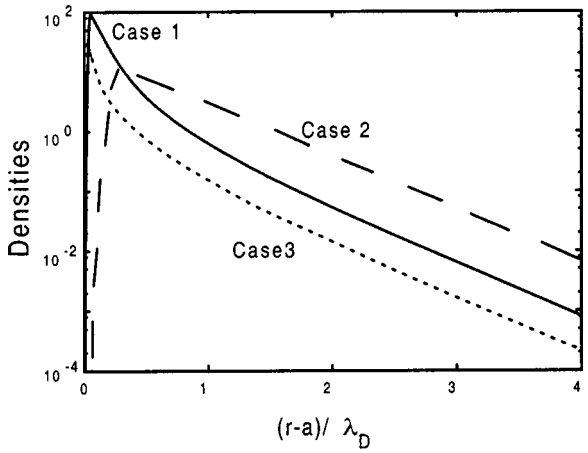


FIG. 6. Trapped ion density $n_t(r)$, scaled to $n_0$, for Case 1 ($a/\lambda_D=0.015$, $T/T_e=0.01$, solid curve), Case 2 ($a/\lambda_D=0.1$, $T/T_e=0.01$, dashed curve), and Case 3 ($a/\lambda_D=0.015$, $T/T_e=0.04$, dotted curve). In all three cases, $\nu\to 0$.

nearly every collision of an untrapped ion at $r<r_T$ results in the creation of a trapped ion, but only a small fraction of the collisions of trapped ions result in the disappearance of a trapped ion. If $T/T_e<a^2/r_T^2$, the trapped ion population falls off because many of the newly born ions have low angular momentum and immediately fall onto the grain. In the opposite limit where $T/T_e$ approaches unity, the trapped ion population again falls off, because many of the newly born ions have enough energy to escape to $r=\infty$. Figure 6 shows the trapped ion density for Case 1 and for two cases with $\nu\to 0$ that test the limits (42). In Case 2, $a/\lambda_D=0.1$ and $T/T_e=0.01$, and in Case 3 $a/\lambda_D=0.015$ and $T/T_e=0.04$. Note that the trapped ion density in these cases is appreciably smaller than in Case 1, where $a/\lambda_D=0.015$ and $T/T_e=0.01$.

In Fig. 7 we plot $r\phi(r)$ for each of the three cases. In Cases 1 and 3, $a/\lambda_D=0.015$ is quite small, and $\phi(r)$ is very close to the simple Debye-shielded potential, out to $r\sim 5\lambda_D$. (For larger $r$, $\phi(r)\sim r^{-2}$. This behavior at large $r$ is due to ion absorption on the grain.[11,4]) In Case 2, where

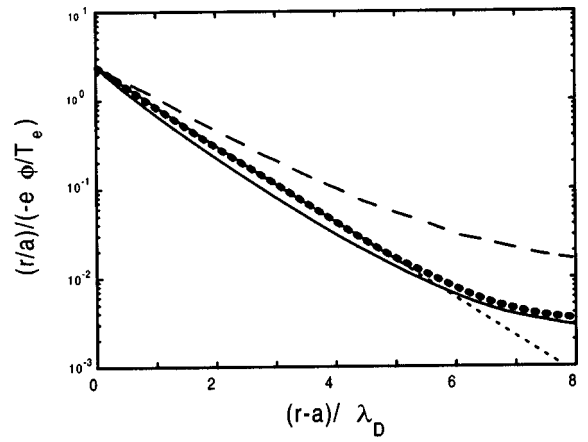


FIG. 7. $r\phi(r)$ for the three cases of Fig. 6. Case 1: solid curve. Case 2: dashed curve. Case 3: heavy dotted curve. The Debye potential is shown as the light dotted line.

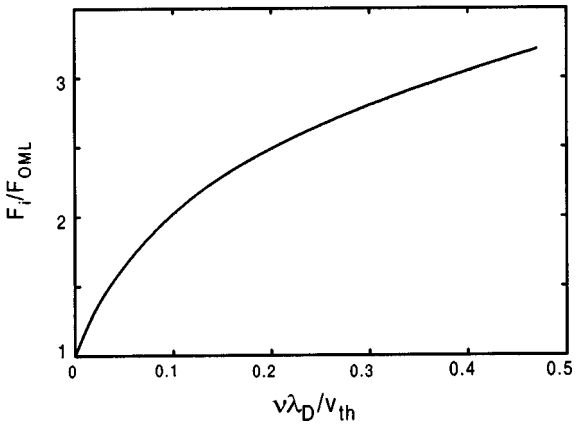


FIG. 8. $F_i/F_{\rm OML}$ as a function of collisionality index $\nu\lambda_D/v_{\rm th}$.

$a/\lambda_D=0.1$ is larger, the potential still shows a Debye-type form out to $r\sim 5\lambda_D$, but with a shielding length that is about 20% larger than $\lambda_D$. In general, the old OML theory (which omits trapped ions) shows Debye-type shielding out to $r\sim 5\lambda_D$, but with a shielding length that is longer than Debye. Including trapped ions in our theory decreases the shielding length, and brings the potential closer to Debye. But for large grains, the OML shielding is significantly weaker than Debye,[2,4] and even with trapped ions remains noticeably weaker than Debye. Actually, it is a bit of a mystery as to why the Debye form works as well as it does, especially when $r<r_T$. The usual derivation of Debye shielding proceeds by linearizing an assumed Boltzmann form for the ion density,

$$n_i(r)=n_0\exp\left(-\frac{e\phi(r)}{T}\right) \tag{43a}$$

$$\simeq n_0\left(1-\frac{e\phi(r)}{T}\right) \tag{43b}$$

and inserting Eq. (43b) and the equivalent expression for electrons into the Poisson equation (21). However, the nonlinear Boltzmann form (43a) is grossly wrong for $r<r_T$; it gives $n_i(r)>e^{100}n_0$ near the grain! The linearization is also completely invalid, as $n_i(r)\gg n_0$ and $|e\phi(r)|\gg T$ near the grain. Nonetheless, the linearized form (43b) works pretty well in deriving the shielded potential from Poisson's equation.

### B. Small but finite collision frequency

For nonzero collision frequency $\nu$, we must determine the floating potential $\phi_f$ by setting the ion flux to the grain $F_i$, from (32) and (36), equal to the electron flux $F_e$ from (25). The determination of $\phi_f$ is done self-consistently with the solution for $n_t(r)$. Figure 8 shows $F_i/F_{\rm OML}$ as a function of the collisionality measure $\nu\lambda_D/v_{\rm th}$, for $a/\lambda_D=0.015$, $T/T_e=0.01$. We see that collisionality increases $F_i$ substantially even when $\nu\lambda_D/v_{\rm th}$ is small. The grain potential $\phi_f$ is shown as a function of $\nu\lambda_D/v_{\rm th}$ in Fig. 9. The floating potential is suppressed by up to 50%, as a result of the collisional increase in ion current to the grain. To a very good

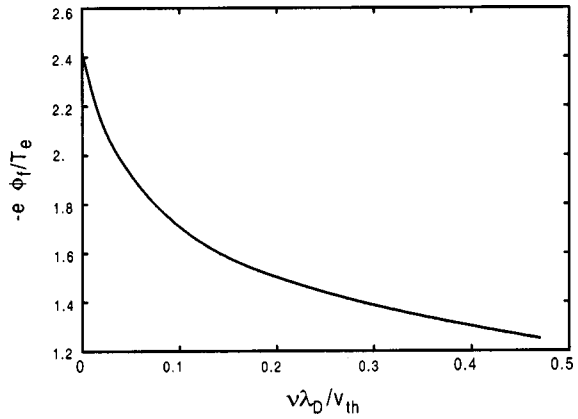


FIG. 9. Floating potential $\phi_f$, as a function of collisionality index $\nu\lambda_D/v_{\rm th}$.

approximation, the charge on the grain is $-Ze=a\phi_f$; thus $Z$ is also reduced by up to 50% as compared to the usually accepted OML value.

It should be noted that there are two contrary effects at work in determining the dependence of $F_i$ on $\nu$. For a specified grain potential $\phi_f$, collisions near the grain strongly increase $F_i$. But collisionality also decreases $|\phi_f|$, and this in turn reduces $F_i$ somewhat. In Fig. 8 we show $F_i$ scaled to the OML ion flux $F_{\rm OML}$ from Eq. (26). Here $F_{\rm OML}$ means the OML flux to a grain whose potential is the OML floating potential given Eq. (27). In some earlier work,[25] we compared $F_i$ to an intermediate benchmark, the OML flux from (26), to a grain whose potential is the full self-consistent value of $\phi_f$, including the effect of collisions. This difference in the definition of $F_{\rm OML}$ explains the apparent difference between Fig. 8 and some of the results quoted in Ref. 25.

In Fig. 10, we show the trapped ion density $n_t(r)$ for several values of $\nu\lambda_D/v_{\rm th}$: Case 1, $\nu\lambda_D/v_{\rm th}\to 0$; Case 4, $\nu\lambda_D/v_{\rm th}=0.037$; Case 5, $\nu\lambda_D/v_{\rm th}=0.47$. In all cases, $T/T_e=0.01$ and $a/\lambda_D=0.015$. Curiously enough, the trapped ion density is seen to *decrease* as $\nu$ increases. This may seem paradoxical since trapped ions are created by collisions. The

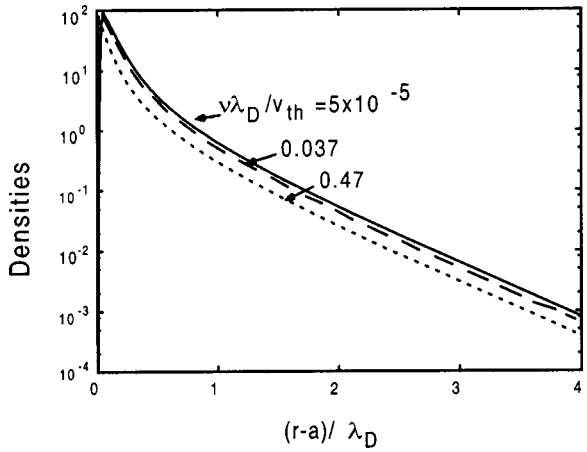


FIG. 10. Trapped ion density $n_t(r)$ for Case 1, $\nu\lambda_D/v_{\rm th}=5\times10^{-5}$ (solid curve); Case 4, $\nu\lambda_D/v_{\rm th}=0.037$ (dashed curve); Case 5, $\nu\lambda_D/v_{\rm th}=0.47$ (dotted curve).

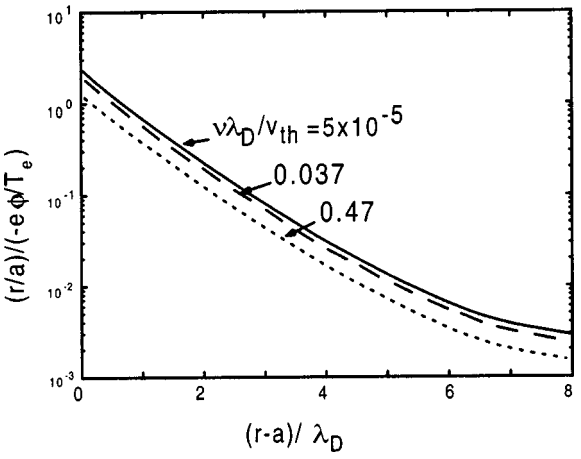


FIG. 11. Potential profile $\phi(r)$ for Case 1, $\nu\lambda_D/v_{\rm th}=5\times10^{-5}$ (solid curve); Case 4, $\nu\lambda_D/v_{\rm th}=0.037$ (dashed curve); Case 5, $\nu\lambda_D/v_{\rm th}=0.47$ (dotted curve).

explanation is that $|\phi_f|$ decreases with increasing collisionality, i.e., the potential well becomes shallower and hence traps fewer ions. We show the complete potential profile $\phi(r)$ for Cases 1, 4, 5 in Fig. 11. In all of these cases $n_t(r)$ significantly exceeds $\Delta n_u(r)$ near the grain, so trapped ions are a dominant factor in shielding.

In Fig. 12, we plot the integrand of Eq. (32), $I(r')\equiv 4\pi r'^2[n_t(r')+n_u(r')]p(r')$. This plot shows the distribution of locations $r'$ where an ion had its last collision before hitting the grain. The result is shown for Case 1, $\nu\lambda_D/v_{\rm th}=5\times10^{-5}$ (i.e., essentially zero, solid curve); Case 4, $\nu\lambda_D/v_{\rm th}=0.037$ (dashed curve); and Case 5, $\nu\lambda_D/v_{\rm th}=0.47$ (dotted curve). This is a log–log plot, so that we can display both the spatial scale $r\sim\lambda_D$ of the sheath and the much longer collisional scale $r\sim v_{\rm th}/\nu$. Note that in all cases there is a peak in $I(r')$ that occurs at $r<\lambda_D$. This is due to the occasional collisions that occur within the sheath. The peak occurs for two reasons: The trapped ion density is very large in this range of $r$, and if a collision occurs within the sheath, the resulting ion is quite likely to hit the grain. The

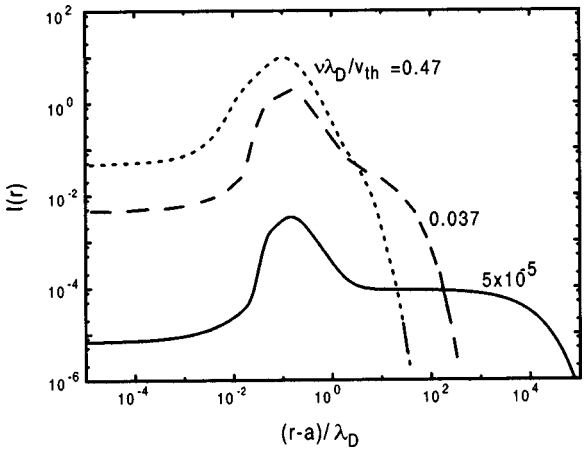


FIG. 12. The integrand $I(r')$ of Eq. (32), for $T/T_e=0.01$, $a/\lambda_D=0.015$, and $\nu\lambda_D/v_{\rm th}=5\times10^{-5}$ (solid curve), $\nu\lambda_D/v_{\rm th}=0.037$ (dashed curve), $\nu\lambda_D/v_{\rm th}=0.47$ (dotted curve). $I(r')$ is the relative contribution to the ion flux to the grain, from collisions at $r'$.

shape of the peak is roughly independent of $\nu$ and the amplitude of the peak is roughly proportional to $\nu$; hence the contribution to $F_i$ is roughly proportional to $\nu$. For the cases $\nu\lambda_D/v_{\rm th}=0.037$ and 0.47, this is the dominant contribution to $F_i$. In addition, $I(r')$ has a broad plateau that extends out to several times the mean free path $v_{\rm th}/\nu$, and then falls off exponentially (because if a collision occurs at such large radius, the resulting ion is likely to have another collision before it can reach the grain). This contribution to $I(r')$ has an amplitude that is proportional to $\nu$, and a spatial range that is inversely proportional to $\nu$; hence its contribution to $F_i$ is independent of $\nu$. This is in fact the OML current. For the cases $\nu\lambda_D/v_{\rm th}=5\times10^{-5}$ and 0.037, the collisional contribution from the peak at $r<\lambda_D$ is clearly distinguished from the OML contribution from the plateau at $r\sim v_{\rm th}/\nu$, but for the cases $\nu\lambda_D/v_{\rm th}=0.47$ the two regimes are beginning to merge. This case pushes the limits of validity of our theory, which assumes $\nu$ to be small.

## V. CONCLUSIONS

We have found that trapped ions created by charge-exchange collisions can dominate both the shielding around a charged grain and the ion current to the grain, which determines the floating potential. In the limit where the collision frequency $\nu\to0$, the trapped ion density in the shielding cloud around the grain can be over an order of magnitude larger than the untrapped ion density. The conditions for the trapped ion density to be large are $T\ll T_e$, so that nearly all the newly created ions are trapped in the potential well, and $a^2/\lambda_D^2\ll T/T_e$, so that very few newly created ions fall immediately onto the grain. For $\nu$ finite but small, the ion current $F_i$ to the grain increases. This increase is roughly proportional to $\nu$, but nonetheless very large. The increased ion flow to the grain suppresses the floating potential $\phi_f$. In the absence of collisions, $e\phi_f$ is typically $-T_e$ to $-3T_e$, but we have seen trapped ion/collisional effects reduce $-e\phi_f$ by as much as 50%. Self-consistently including this reduction in the well depth reduces the density of trapped ions slightly; thus the trapped ion density is actually largest in the limit $\nu\to0$.

The presence of a large population of trapped ions profoundly changes the nature of the interaction of a grain with other grains, and with external forces. We have previously argued[4] that shielding by untrapped ions cannot lead to a net attractive electrostatic force between negatively-charged grains. But a grain with its trapped ion cloud can behave like a ''classical atom;'' the trapped ion cloud can be polarized, thereby shielding the grain from electric fields,[2,17] and possibly leading to van der Waals type attractive forces between grains. We are studying these effects at the present time.

This paper has been concerned with trapped ion and collisional effects for a spherical dust grain which is at floating potential. It has recently been shown,[26,27] both theoretically and experimentally, that the same effects can also be important in connection with the ion current to a cylindrical Langmuir probe, either biased or floating.

## ACKNOWLEDGMENTS

M.L. wishes to thank Dr. Wallace Manheimer for contributing some good ideas early in the work.

The work of M.L., R.G., V.G., G.G., and G.J. was supported by the Office of Naval Research and NASA. The work of Z.S. and S.R. was supported by the Office of Fusion Energy Sciences of the Department of Energy.

## APPENDIX: VALIDITY OF THE OML ASSUMPTION (NO POTENTIAL BARRIERS)

If the effective potential $U(r;J)$, defined in Eq. (2), has a maximum $U_{\rm max}>0$ which occurs at $r=r_m$, then phase space for ions with angular momentum J and energy $\epsilon<U_{\rm max}$ is partitioned into two regions: trapped ions for $r<r_m$, and untrapped ions for $r>r_m$. There are no collisionless trajectories connecting the two regions, so it is possible that the distribution function has a different form in each region. We have avoided significant mathematical complications by assuming that there are no such barriers, or more precisely that if there is a maximum in $U(r)$ it is so low or occurs in such a limited range of $J$ that it affects a negligible number of ions. It follows then that trapped ions are simply synonymous with negative-energy ions.

The neglect of centrifugal potential barriers has a long history, and is one of the key assumptions of the orbital-motion-limited (OML) theory of probes. There has been renewed interest recently in the question of validity of this assumption. Bernstein and Rabinowitz[11] showed long ago that in the limit $a\ll\lambda_D$, there are no potential barriers if the ambient ion distribution is monoenergetic. It was generally assumed, over the years, that potential barriers could be neglected if $a\ll\lambda_D$, even if the distribution is Maxwellian. However, Allen, Annaratone and de Angelis[5] showed recently that for a Maxwellian distribution, there are always some ions subject to potential barriers, even if $a/\lambda_D$ is small. We subsequently calculated[6,7] the actual magnitude of the potential barriers, under the assumption that $\phi(r)$ has the Debye form,

$$\phi(r)=\phi_f\frac{a}{r}e^{-r/\lambda_D}, \tag{A1}$$

at least for $r$ out to several $\lambda_D$. As we have seen in Sec. IV, Eq. (A1) appears to be a good qualitative approximation, so it forms a reasonable basis for estimating the effect of potential barriers. We concluded in Ref. 6 that the most significant potential barriers occur for $J$ in the range,

$$\frac{1}{2}a\lambda_D\phi_f<\frac{J^2}{m}<\frac{3}{4}a\lambda_D\phi_f, \tag{A2}$$

where $U(r)$ does indeed have a maximum $U_{\rm max}$ and the value of the maximum is in the range

$$0.01\frac{a}{\lambda_D}\frac{e|\phi_f|}{T}<\frac{U_{\rm max}}{T}<0.02\frac{a}{\lambda_D}\frac{e|\phi_f|}{T}. \tag{A3}$$

Only a fraction of order $0.01(a/\lambda_D)|e\phi_f/T|$ of those ions whose angular momentum satisfies (A2) are stopped by the potential barrier. Although $|e\phi_f/T|$ is a large quantity ($\phi_f$

$\sim -T_e$ to $-3T_e$, which can be >100T), $a/\lambda_D$ is typically small in dusty plasmas, and in most cases only a small fraction of the ions are reflected at the barrier.

There is an additional consideration that limits the number of trapped ions that can be reflected by a potential barrier. Consider an ion newly created by a collision at $r'$. The typical value of $J^2$ is $mr'^2T$, and thus condition (A2) can be estimated as

$$\frac{1}{2}\frac{a}{\lambda_D}\frac{e|\phi_f|}{T}<\frac{r'^2}{\lambda_D^2}<\frac{3}{4}\frac{a}{\lambda_D}\frac{e|\phi_f|}{T}, \tag{A4}$$

$U_{\max}$ is large enough to reflect a substantial number of ions only in cases where

$$\frac{a}{\lambda_D}\frac{e|\phi_f|}{T}>20. \tag{A5}$$

In these cases, Eq. (A4) reduces approximately to

$$3<\frac{r'}{\lambda_D}<4. \tag{A6}$$

So even in those unusual cases where the barrier is fairly strong, its primary effect is to trap a few ions with slightly positive energy, created in a limited spatial region. In essence, the potential barrier slightly alters the perimeter of the potential well. Neglecting the effect of potential barriers generally appears to be quite a reasonable approximation for dusty plasmas.


[1] E. C. Whipple, Rep. Prog. Phys. **44**, 1197 (1981).
[2] J. E. Daugherty, R. K. Porteus, M. D. Kilgore, and D. B. Graves, J. Appl. Phys. **72**, 3934 (1992).
[3] C. K. Goertz, Rev. Geophys. **27**, 271 (1989).
[4] M. Lampe, G. Joyce, G. Ganguli, and V. Gavrishchaka, Phys. Plasmas **7**, 3851 (2000).
[5] J. E. Allen, B. M. Annaratone, and U. deAngelis, J. Plasma Phys. **63**, 299 (2000).
[6] M. Lampe, J. Plasma Phys. **65**, 171 (2001); J. E. Allen, J. Tech. Phys. **43**, 241 (2002).
[7] M. Lampe, G. Joyce, G. Ganguli, and V. Gavrishchaka, Phys. Scr., T **89**, 106 (2001).
[8] J.-P. Boeuf and C. Punset, in *Dusty Plasmas*, edited by A. Bouchoule (Wiley, New York, 1999), Chap. 1, p. 9.
[9] H. Mott-Smith, Jr. and I. Langmuir, Phys. Rev. **28**, 27 (1926).
[10] J. E. Allen, R. L. Boyd, and P. Reynolds, Proc. Phys. Soc. London, Sect. B **70**, 297 (1957).
[11] I. B. Bernstein and I. N. Rabinowitz, Phys. Fluids **2**, 112 (1959).
[12] F. F. Chen, J. Nucl. Energy, Part C **7**, 47 (1965).
[13] J. G. Laframboise, University of Toronto, Institute For Aerospace Studies, Report No. 100 (1966). Copies are available from the UT-IAS library.
[14] J. G. Laframboise and L. W. Parker, Phys. Fluids **16**, 629 (1973).
[15] J. E. Allen, Phys. Scr. **45**, 497 (1992).
[16] B. M. Annaratone, M. W. Allen, and J. E. Allen, J. Phys. D **25**, 417 (1992) noted that if the grain is large enough, collisions at a distance of order one mean free path from the grain can cause ions to fall directly onto the grain, thereby effecting a transition from the OML theory to the radial inflow theory of Allen, Boyd, and Reynolds (Ref. 10). See also Ref. 12. This effect is included in the present work, as well as the additional effect of orbiting trapped ions created by collisions.
[17] J. Goree, Phys. Rev. Lett. **69**, 277 (1992).
[18] A. V. Zobnin, A. P. Nefedov, V. A. Sinel'shchikov, and V. E. Fortov, JETP **91**, 483 (2000).
[19] M. Lampe, V. Gavrishchaka, G. Ganguli, and G. Joyce, Phys. Rev. Lett. **86**, 5278 (2001).
[20] Properly speaking, charge-exchange collisions are elastic scatterings by 180° in the center-of-mass frame. For fast ions, there is a pronounced peak in the differential scattering cross section at 180°, as shown by M. L. Vestal, C. R. Blakley, and J. H. Futrell, Phys. Rev. A **17**, 1337 (1978). Thus charge-exchange is clearly the dominant ion collision. The differential cross section is less peaked for ion energy below 1 eV, and it becomes more difficult to distinguish charge-exchange from other elastic scattering. However, for purposes of creating and destroying trapped ions, clearly charge-exchange collisions have the greatest effect. Elastic and ion–ion collisions also result in energy loss and pitch-angle scattering of an incoming fast ion, and we believe that including these types of collisions would in effect slightly increase the collision frequency without qualitatively changing the results. A comprehensive discussion of the role of these different types of collisions is given by A. V. Phelps, J. Appl. Phys. **76**, 747 (1994).
[21] The energy dependence of charge-exchange cross sections is given by R. Hegerberg, M. T. Elford, and H. R. Skullerud, and summarized by M. A. Lieberman and A. J. Lichtenberg, *Principles of Plasma Discharges and Materials Processing* (Wiley, New York, 1994), p. 78. In general (depending on the specific gas), the energy dependence is somewhere between constant cross-section and constant collision frequency.
[22] We recall here that we have assumed $U(r)$ has no maxima, and consequently that all trapped ions have negative energy. In reality, $U(r)$ has very weak maxima that permit a small number of ions with small positive energy to be trapped at $r>r_1$. The neglect of these trapped ions is usually of little consequence, as discussed in the Appendix.
[23] G. L. Natanson, Zh. Tekh. Fiz. **30**, 573 (1960) [Sov. Phys. Tech. Phys. **30**, 573 (1960)].
[24] An ion that hits the grain will have energy of order $T_e$ at impact. Therefore its angular momentum can be no larger than order $a(2T_e/m)^{1/2}$. If this ion starts at $r=\lambda_{\rm mfp}$ with thermal energy of order $T$, angular momentum conservation indicates that $\sin^2\theta<(a/\lambda_{\rm mfp})^2(T_e/T)$. Normally $a/\lambda_{\rm mfp}<10^{-2}$, so $\theta\ll 1$.
[25] M. Lampe, G. Ganguli, V. Gavrishchaka, R. Goswami, and G. Joyce, "Collisional and nonlinear effects on grain charge and intergrain force," in *Proceedings of the Third International Conference on Physics of Dusty Plasmas*, Durban, South Africa, May 2002, AIP Conf. Proc. **649**, 357 (2002).
[26] Z. Sternovsky and S. Robertson, Appl. Phys. Lett. **81**, 1961 (2002).
[27] Z. Sternovsky, S. Robertson, and M. Lampe, Phys. Plasmas **10**, 300 (2003).